Citation: Molecular Therapy — Methods & Clinical Development (2016) **5,** 16009; doi:10.1038/mtm.2016.9
Official journal of the American Society of Gene & Cell Therapy

www.nature.com/mtm

ARTICLE

Development of a real-time imaging system for hypoxic cell apoptosis

Go Kagiya[1], Ryohei Ogawa[2], Fuminori Hyodo[3], Kei Yamashita[4], Mizuki Nakamura[5], Ayumi Ishii[6], Yukihiko Sejimo[7], Shintaro Tominaga[1], Masaharu Murata[3], Yoshikazu Tanaka[8] and Masanori Hatashita[8]

Hypoxic regions within the tumor form due to imbalances between cell proliferation and angiogenesis; specifically, temporary closure or a reduced flow due to abnormal vasculature. They create environments where cancer cells acquire resistance to therapies. Therefore, the development of therapeutic approaches targeting the hypoxic cells is one of the most crucial challenges for cancer regression. Screening potential candidates for effective diagnostic modalities even under a hypoxic environment would be an important first step. In this study, we describe the development of a real-time imaging system to monitor hypoxic cell apoptosis for such screening. The imaging system is composed of a cyclic luciferase (luc) gene under the control of an improved hypoxic-responsive promoter. The cyclic luc gene product works as a caspase-3 (cas-3) monitor as it gains luc activity in response to cas-3 activation. The promoter composed of six hypoxic responsible elements and the CMV IE1 core promoter drives the effective expression of the cyclic luc gene in hypoxic conditions, enhancing hypoxic cell apoptosis visualization. We also confirmed real-time imaging of hypoxic cell apoptosis in the spheroid, which shares properties with the tumor. Thus, this constructed system could be a powerful tool for the development of effective anticancer diagnostic modalities.

Molecular Therapy — Methods & Clinical Development (2016) **5**, 16009; doi:10.1038/mtm.2016.9; published online 2 March 2016

INTRODUCTION

Apoptosis is responsible for many normal developmental and physiological processes.[1] Its deficiency often leads to carcinogenesis. Caspases, a family of cysteine proteases, play an essential mediator role in mammalian cells. Caspase-3 (cas-3) is activated in apoptotic cells through death ligand and mitochondrial pathways and consequently recognizes and cleaves the DEVD peptide sequence (N-Asp-Glu-Val-Asp-C) on the carboxy side of the second aspartic acid residue. Once activated, cas-3 is responsible for the proteolytic cleavage of a broad spectrum of cellular targets, which ultimately leads to cell death.[2,3]

Development of an imaging system to noninvasively detect caspase activity is considered to be an interesting approach for screening of novel anticancer drugs because apoptosis induction by the drugs exerts a curative influence on cancer. Hence, several unique methods to monitor apoptosis have been developed to date. Among these methods, Ozawa and colleagues[4] have successfully constructed a noninvasive real-time imaging system to detect apoptosis in transplanted tumor tissue on nude mice. They utilized a cyclic luc system in which two-halves of fragmented luc genes were connected in the inverse order with a DNA fragment coding for the DEVD peptide sequence, in addition to DNA fragments coding for a DnaE intein placed at the 5′ and 3′ end of the reconnected luc gene. A polypeptide translated from this entire DNA fragment is circularized with protein splicing activity of the DnaE intein placed at both ends. Although the cyclic luc distorted by the ligation of both terminals loses its enzymatic activity, the noncyclic luc formed as a result of cleavage at the DEVD motif by cas-3 during the apoptotic process was restored to the wild-type structure and regained its enzymatic activity, enabling noninvasive real-time imaging of apoptosis in cells transfected with this system.

Solid tumor is highly heterogeneous in terms of oxygenation and contains hypoxic cell regions as a result of an imbalance between cell proliferation and angiogenesis; specifically, temporary closure or a reduced flow due to abnormal vasculature.[5,6] As the primary cellular and systemic response to hypoxic stress, tumor cells in such regions induce the production of hypoxia-inducible factors (HIFs), master transcription regulators that consist of two different protein molecules, a HIFα subunit and a HIFβ subunit.[7,8] HIF-1α, one of HIF-α family members, is constitutively expressed. In addition, although HIF-1β is unaffected by changes in the cellular oxygen concentrations, HIF-1α accumulation is O_2 dependently regulated.[7–9] Under normoxic conditions, HIF-1α is constantly degraded via hydroxylation of proline residues within its oxygen-dependent

[1]School of Allied Health Sciences, Kitasato University, Sagamihara, Kanagawa, Japan; [2]Department of Radiological Sciences, Graduate School of Medicine and Pharmaceutical Sciences, University of Toyama, Sugitani, Toyama, Japan; [3]Innovation Center for Medical Redox Navigation, Kyushu University, Higashi-ku, Fukuoka, Japan; [4]Division of Radiation Oncology, Chiba Cancer Center, Chiba, Chiba, Japan; [5]Department of Diagnostic Radiology, Kitasato University Hospital, Sagamihara, Kanagawa, Japan; [6]Department of Diagnostic Radiology, Saitama Prefectural Cancer Center, Kitaadachi-gun, Saitama, Japan; [7]Graduate School of Medicine, Gunma University, Maebashi, Gunma, Japan; [8]Biology Group, The Wakasa Wan Energy Research Center, Nagatani, Tsuruga, Fukui, Japan. Correspondence: Ryohei Ogawa (ogawa@med.u-toyama.ac.jp)
Received 24 November 2015; accepted 13 January 2016;

degradation domain by prolyl hydroxylases and the von Hippel Lindau protein-mediated ubiquitin–proteasome pathway. However, under hypoxia, reactive oxygen species (ROS) are generated by the mitochondrial electron transport chain and then released to the cytosol, thereby leading to stabilization of HIF-1α through prolyl hydroxylases inhibition due to oxidation of Fe^{2+} within prolyl hydroxylases.[10] The stabilized HIF-1α subunit is translocated into the nucleus, where it forms a heterodimeric transcriptional complex with HIF-1β subunit and directly binds to the hypoxia-responsive element (HRE, 5′-A/GCGTG-3′) to express a number of its target genes involved in angiogenesis, metabolic adaptation, tolerance of acidosis, cell survival, and metastasis.[11–14] As a result, the expression of HIF-1 facilitates tumor cell survival and growth in hypoxic regions.

In cancer therapy, anticancer drugs and ionizing radiation enhance cell-killing effects by targeting DNA in proliferating tumor cells. On the other hand, hypoxic cells show greater resistance to these treatments than cells in normoxic regions because these cells display low levels of proliferation in the quiescent state (slow cycling or G0) and exist in the microenvironment where the oxygen effect of ionizing radiation is reduced.[15,16] Therefore, hypoxic cells demonstrate a higher possibility of surviving through these treatments than normoxic cells in the tumor tissues, potentially resulting in metastasis or recurrence. In other words, treatments targeting hypoxic cells appear to be a promising strategy for eliminating cancer. To date, nitroimidazole compounds, such as misonidazole, pimonidazole, and nimorazole have been synthesized as hypoxic cell radiosensitizers causing hypoxic tumor cells to become more sensitive to radiation therapy, and these agents have subsequently been tested in clinical trials. Although these drugs exhibit significant radiosensitizing effects *in vitro*, they show low levels of radiosensitization *in vivo* and introduce harmful side-effects, including peripheral neuropathy.[17] In recent years, bioreductive prodrugs have also been actively developed as novel hypoxia-targeted drugs. In particular, tirapazamine (3-amino-1,2,4-benzotriazine 1,4-dioxide, TPZ), which induces damage to hypoxic cells by reactive oxygen species produced following one-electron reduction by cytochrome P(450) reductase-enriched microsomes, is currently undergoing evaluation in phase 3 clinical trials.

At present, the development of therapeutic approaches targeting the hypoxic cells is one of the most urgent and crucial challenges for cancer eradication. A noninvasive real-time imaging system to monitor hypoxic cell apoptosis could be a useful tool for screening novel anticancer drugs that enhance hypoxic cell-killing effects and to evaluate therapeutic approaches targeting the hypoxic cells. In this study, we constructed a real-time imaging system for apoptotic cells induced under hypoxic conditions, taking advantage of the cyclic luc system under control of the hypoxia-responsive promoter.

RESULTS

Construction of the hypoxic-responsive promoter for the expression of the cyclic luc gene

The cyclic luc system developed by Ozawa and colleagues could be useful for noninvasively imaging of apoptosis induced in hypoxic regions when its expression is regulated by the hypoxia-responsive promoter (Figure 1). First, we reproduced the construct of the cyclic luc system and placed the DNA fragment under control of the cytomegalovirus (CMV) promoter to construct plasmid CMV (pCMV) plasmids (Figure 2a). Cells transfected with the plasmids successfully produced a chemiluminescent signal after treatment with 1 μmol/l staurosporine (STS), used as an apoptosis inducing agent, for 2 hours under general cell culture conditions or a hypoxic condition. We then employed the HREs and connected them to the TATA box to construct a hypoxia-responsive promoter and replaced the CMV promoter of pCMV with the constructed promoters. To obtain optimum inducibility of the gene expression in response to hypoxia, we constructed plasmids,

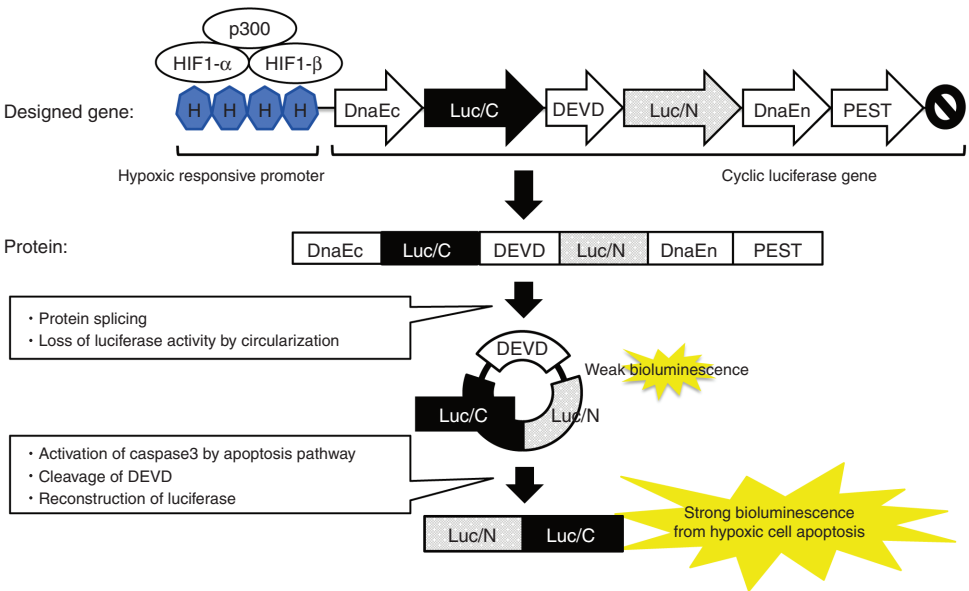

Figure 1 A schematic illustration for the detection of hypoxic cell apoptosis utilizing cyclic luc. The expression of the cyclic luc gene is regulated by HIF-1, a heterodimeric DNA binding complex composed of HIF-1α and HIF-1β. Upon translation, the DnaEc and DnaEn inteins interact with one another to catalyze protein splicing to circularize the polypeptide. Failure in this event yields rapid degradation due to the PEST domain of a signal peptide for protein degradation. The cyclic luc distorted by circularization loses its enzymatic activity. However, the cyclic luc restores its authentic structure when cleaved at the DEVD peptide by cas-3 during apoptosis, producing high chemiluminescence by luciferin oxidation. H: HRE, DnaEn: N-terminal fragment of DnaE intein, DnaEc: C-terminal fragment of DnaE intein, Luc/N: N-terminal fragment of firefly luc, Luc/C: C-terminal fragment of firefly luc.

p4HREs, p6HREs, and p12HREs, containing 4, 6, and 12 tandemly repeated copies of HRE upstream of the TATA box, respectively, and subjected the cells to a luc induction assay under either normoxic or hypoxic conditions. Although cells transfected with p4HREs, p6HREs or p12HREs were treated with 1 μmol/l STS for 2 hours, no construct produced a chemiluminescent signal under normoxic condition. However, under hypoxic conditions, chemiluminescent signals were detected in all the transfectants. Among them, cells transfected with p6HREs showed the strongest signal with the greatest difference in the signal strengths between with or without STS (Figure 2b). In addition, we also confirmed that in the presence of 100 μmol/l $CoCl_2$, a hypoxic mimicking agent, cells transfected with p6HREs showed the highest chemiluminescent signal after treatment with 1 μmol/l STS among cells transfected with the constructed plasmid. These results show that the cyclic luc gene under control of the hypoxia-responsive promoter could be used to detect apoptotic cells only under hypoxic conditions. Particularly, p6HREs, a plasmid containing a promoter which is composed of six HREs and the TATA box, showed the most promising result. To determine if the system could be applied in other cell types, we then employed Chang liver cells that are tumorigenic on a nude mouse, in addition to COS-7 cells. When we identically treated Chang liver cells carrying p6HREs with STS, we obtained a similar result in terms of the induction

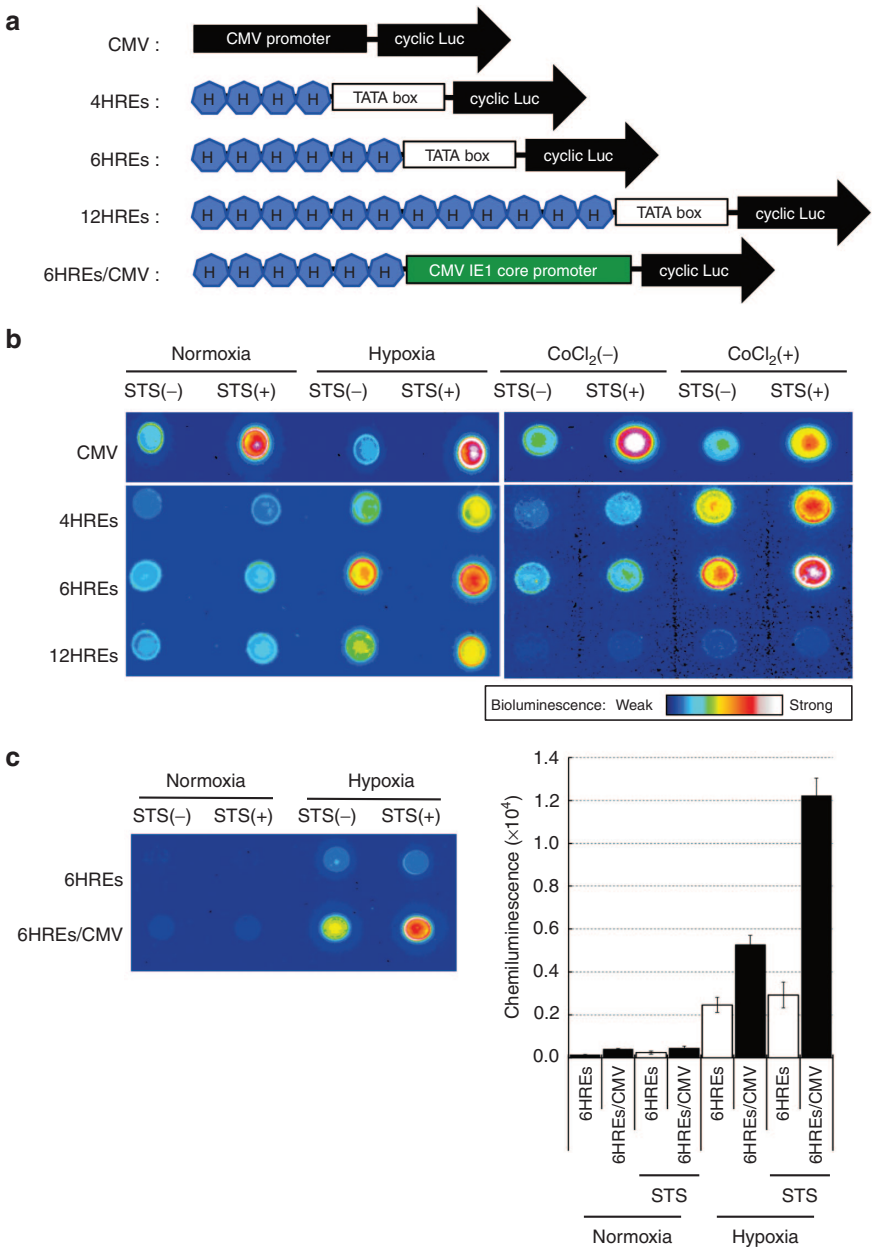

Figure 2 Constructions of hypoxic-responsive promoters for the expression of the cyclic luc gene in hypoxic conditions. (**a**) Schematic representations of the constructed promoters. "H" in the septangle represents a hypoxia-responsive element. (**b**) Evaluation of the constructed promoters for hypoxia-specific chemiluminescent signals in response to STS treatment in COS-7 cells. Transiently transfected cells with plasmid 4HREs, 6HREs or 12HREs were incubated under hypoxia (0.1% O_2) or with 100 μmol/l $CoCl_2$ and then treated with or without 1 μmol/l STS for 2 hours before chemiluminescent imaging of cell extracts from each sample. (**c**) Evaluation of 6HREs/CMV, an improved promoter, in Chang liver cells transiently transfected with p6HREs or p6HREs/CMV in similar experiments to that in **b**. Digitizing chemiluminescence intensities were plotted in the bar graph ($n = 5$, mean ± SD).

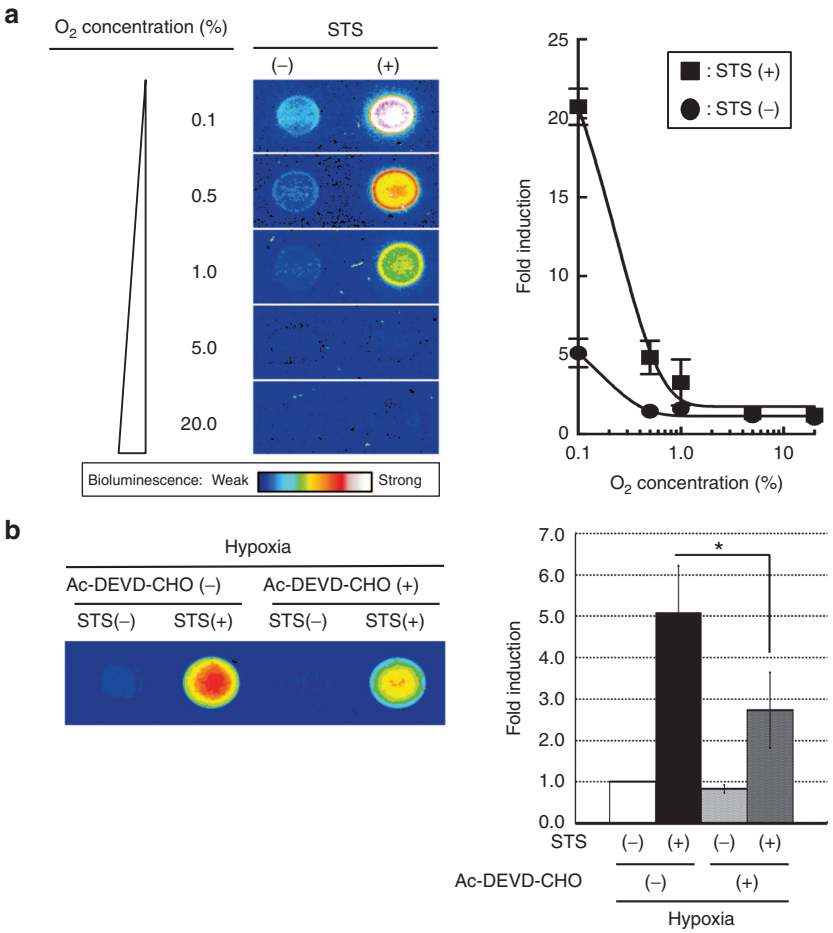

Figure 3 Characterization of p6HREs/CMV, a hypoxic cell apoptosis sensor plasmid, in Chang liver cells. (**a**) Oxygen concentration dependency of chemiluminescence from apoptotic cells. Chang liver cells transiently transfected with p6HREs/CMV were incubated for 12 hours at different O_2 concentrations (0.1, 0.5, 1.0, 5.0, and 20%) and then treated with 1 µmol/l STS for 2 hours at each O_2 concentration for chemiluminescent imaging. The fold inductions were calculated by dividing the chemiluminescent values of the harvested extracts from cells incubated at corresponding O_2 concentrations with or without STS by the chemiluminescent value of extracts at 20% O_2 concentration without STS ($n = 5$, mean ± SD). (**b**) Suppression of chemiluminescence by the cas-3 inhibitor Ac-DEVD-CHO. Chang liver cells transiently transfected with p6HREs/CMV were pre-incubated under hypoxia (0.1% O_2) for 12 hours and then treated with 1 µmol/l STS for 2 hours after incubating the cells in medium containing 100 µmol/l Ac-DEVD-CHO for 1 hour before chemiluminescent imaging. The fold inductions were calculated by dividing the chemiluminescent values of the harvested extracts of cells treated with or without STS and with or without Ac-DEVD-CHO by that of cells without any treatment under hypoxia (0.1% O_2). The asterisks indicate statistical significance (paired Student's *t*-test, $P < 0.05$; ($n = 5$, mean ± SD).

ratio of the cyclic luc gene expression under hypoxic conditions. However, the strength of the signals was four times lower as a whole than those observed in COS-7 cells. This made it difficult to capture real-time images of hypoxic cell apoptosis. Thus, we improved the promoter by replacing the TATA box of p6HREs with the CMV IE1 core promoter to construct p6HREs/CMV. This improved promoter enhanced the expression of the cyclic luc gene and the strength of the signals in hypoxia up to four times at 2 hours after 1 µmol/l STS treatment (Figure 2c)

Oxygen concentration and cas-3 dependent chemiluminescence by p6HREs/CMV

To evaluate O_2 concentration dependency of p6HREs/CMV, we measured chemiluminescent signals in response to 1 µmol/l STS treatment in transfected Chang liver cells with the plasmid at different O_2 concentrations (0.1, 0.5, 1.0, 5.0, and 20%). As shown in Figure 3a, the fold induction of the chemiluminescent signal at 0.1% O_2 was the highest among those we examined. It decreased at increasing O_2 concentrations when the cells were treated with or without STS. However, significant differences between cell cultures treated with or without STS were observed at a range of O_2 concentrations between 0.1 and 1%, confirming that the constructed system could readily detect apoptosis specifically under hypoxia, because the median value of the oxygen partial pressure in tumor tissue is ~1.3%.[6] Moreover, we then performed visualization of cells treated with or without STS under hypoxia in the presence and absence of Ac-DEVD-CHO, a cas-3 inhibitor, to confirm that visualization was cas-3 dependent. The caspase inhibitor significantly decreased the chemiluminescence signals of cells treated with STS, confirming that visualization of the cells with chemiluminescence was induced by cleavage of the cyclic luc gene product due to cas-3 activation (Figure 3b).

Chemiluminescent imaging of hypoxic cell apoptosis induced by various anticancer agents

We then used other anticancer agents to determine if the constructed system could also work to visualize hypoxic cell apoptosis *in vitro*. To do this, we constructed CMV-cLuc and 6HREs/CMV-cLuc cell lines

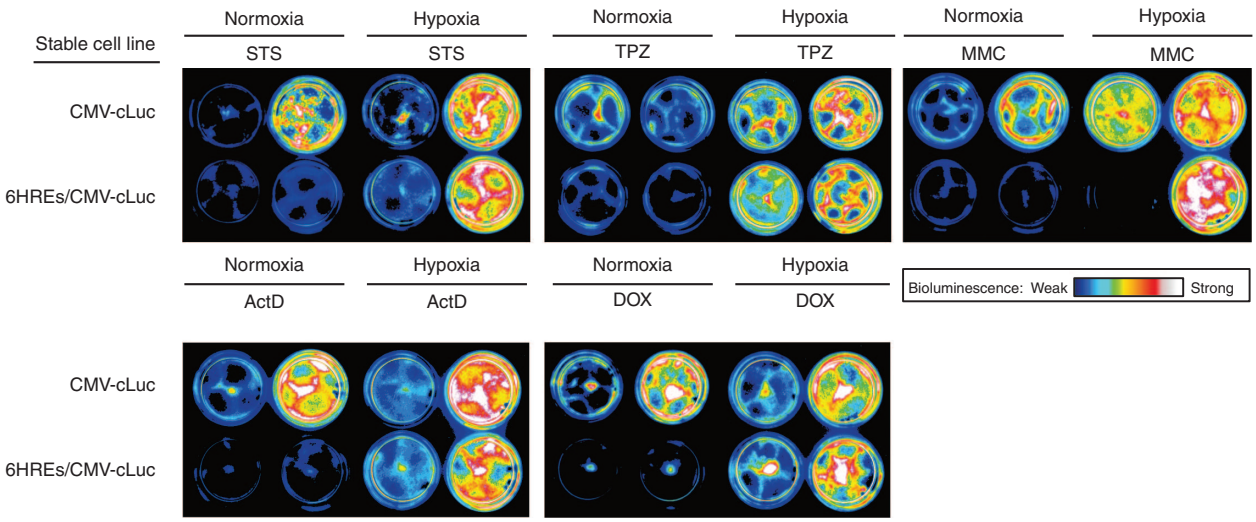

Figure 4 Chemiluminescent images of apoptosis induced by various anticancer agents. CMV-cLuc and 6HRE-/CMV-cLuc transfected cells were incubated for 12 hours under hypoxia (0.1%O_2) and then treated with 1 µmol/l STS for 2 hours, 20 µmol/l TPZ for 24 hours, 60 µmol/l mitomycin C for 8 hours, 200 nmol/l actinomycin D for 6 hours or 8 µmol/l doxorubicin for 8 hours under hypoxia (0.1% O_2 or 1.0% O_2 in TPZ treatment) before chemiluminescent imaging with a lumino image analyzer.

stably transfected with pCMV and p6HREs/CMV, respectively. Upon treatment with various anticancer agents, such as staurosporine (STS), tirapazamine (TPZ), mitomycin C, actinomycin D and doxorubicin, CMV-cLuc clearly increased the chemiluminescent signals under both normoxia and hypoxia regardless of the oxygen concentration; however, this result was not observed with TPZ treatment, an experimental anticancer agent that is activated to a toxic radical specifically under hypoxia. Conversely, 6HREs/CMV-cLuc treated with the same anticancer agents increased chemiluminescent signals only under hypoxic conditions (Figure 4). These results indicate that synthesized product from the cyclic luc gene under control of 6HREs/CMV activated the enzyme activity of luc to visualize apoptotic cells induced with various anticancer drugs only under hypoxic conditions.

Chemiluminescent imaging of apoptotic cells induced in the hypoxic region inside the spheroid

A spheroid can be regarded as an *in vitro* model of tumor because it exhibits marked similarity to the microenvironment of tumors *in vivo*, including oxygen and nutrient concentrations, glycometabolism, and the expression of receptors on the cell surface.[18] We thus took advantage of the properties of the spheroid to visualize apoptotic cells induced in the hypoxic region inside the spheroid. To confirm the presence of hypoxic regions inside the spheroid, we added LOX-1 to the culture medium after formation of spheroids of 6HRE-/CMV-cLuc by incubation in a 3D cell-culture plate for 20 days. LOX-1, which is an iridium compound capable of emitting red phosphorescence under hypoxia, enables the detection of hypoxic regions by observation with conventional fluorescence microscopes without complicated procedures, such as immunohistochemical detection with pimonidazole.[19] Therefore, LOX-1 was used as a hypoxia probe in this study. As shown in Figure 5a, regions inside formed spheroids stained with bright red fluorescence, indicating the presence of hypoxic regions. In addition, we examined the accumulation of HIF-1α in the spheroid culture cells by a western blot analysis. As shown in Figure 5b, HIF-1α accumulations were detected in monolayer cell cultures of stable cell lines under hypoxic conditions, but not normoxic conditions. However, in the spheroid culture condition, HIF-1α accumulations were observed in both cell lines even under normoxic conditions. We thus assessed our system for visualization of hypoxic apoptosis of the spheroid cultures. As shown in Figure 5c, intense fluorescent signals in the spheroids were observed after treatment of 6HRE-/CMV-cLuc with 1 µmol/l STS for 2 hours. However, without STS treatment, much less fluorescence was observed. The obtained result suggests that our constructed system could be applied for *in vivo* imaging of hypoxic cell apoptosis.

DISCUSSION

In this study, we described that the cyclic luc system under control of a HRE-based promoter produced chemiluminescence in various cell types in a cas-3 dependent manner only under hypoxic conditions. In addition, in Chang liver cells mainly used in this study, a hypoxia-responsive promoter composed of six copies of HRE and the CMV IE1 core promoter was the best in responding to hypoxia among constructed promoters containing different numbers of HRE copies, enhancing the chemiluminescence intensity up to 31-fold in response to hypoxia and STS. Furthermore, we showed that the chemiluminescence intensity was dependent of O_2 concentration. The Chang liver cell line stably transfected with this constructed system visualized apoptosis induced by various anticancer agents only in hypoxia. Kaluz *et al.* constructed a hypoxia-responsive promoter containing four copies of HRE after investigating the effects of changing bases in the wild-type HRE sequence residing upstream of the mPKG1 gene or the mLDHA gene, in addition to the distances between HREs and between HRE and the TATA box.[20] According to their findings, we constructed a hypoxia-responsive promoter containing four HREs and confirmed its strong response to hypoxia. We added more HREs to the promoter and found one containing six copies showed the strongest response to hypoxia among the plasmids constructed. Under a hypoxia mimic condition with $CoCl_2$, similar results were obtained. A transcription factor complex consisting of HIF-1α and HIF-1β binds to one copy of HRE.[21] Therefore, the numbers of the transcriptional complex binding to six copies of HRE are more than that of the promoter with four HREs. This may explain the improved response to hypoxia by the inclusion of six HREs. The reason for the inferior response of 12 HREs to hypoxia remains

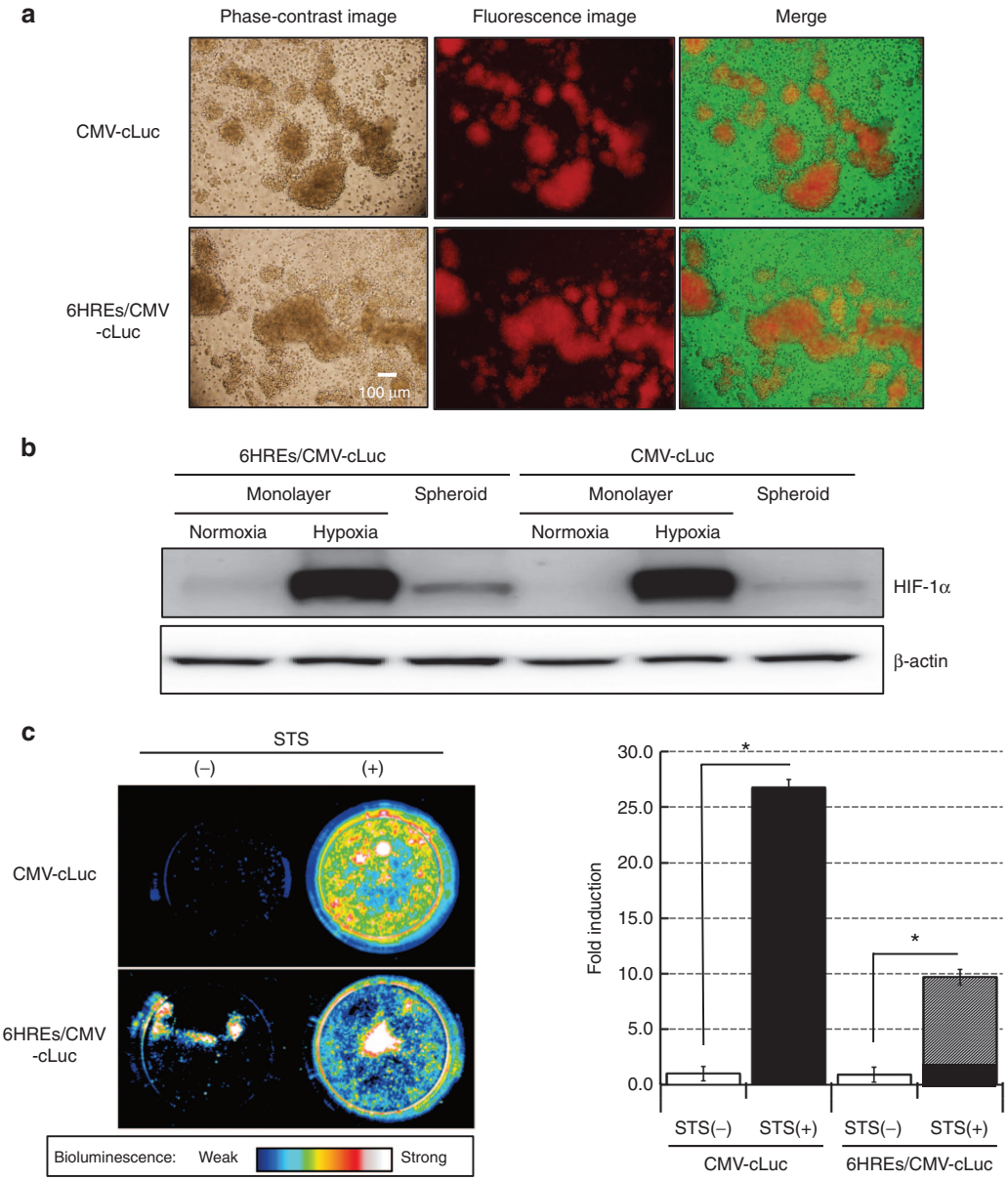

Figure 5 Chemiluminescent imaging of apoptotic cells induced specifically in the hypoxic region of the spheroid formed with 6HRE-/CMV-cLuc transfected cells. (**a**) Distributions of hypoxic regions in the spheroid. Hypoxic regions stained red with LOX-1. Colocalization of spheroids and hypoxic regions were shown by merging of a fluorescent image into its phase construct image. (**b**) The accumulation of HIF-1α inside the spheroids. Spheroids or monolayer cultures of CMV-cLuc and 6HRE-/CMV-cLuc transfected cells were harvested for a western blot analysis of the HIF-1α protein. β-actin served as the loading control. (**c**) Chemiluminescent imaging of hypoxic cell apoptosis in the spheroids. The spheroids were treated with 1 μmol/l STS for 2 hours and then chemiluminescent imaging was acquired with a lumino image analyzer. Chemiluminescent values were measured by a luminometer and the fold induction was calculated to plot the bar graph. The asterisks indicate statistical significances in the comparisons between samples treated with and without STS (paired Student's *t*-test, $P < 0.01$; $n = 5$, mean ± SD).

unknown. Excess numbers of tandemly repeated HRE copies may affect its conformation, possibly interfering with binding of HIF. Although a cas-3 monitoring plasmid, p6HREs containing six copies of HRE and the TATA box, showed strong chemiluminescence in COS-7 cells, the signal was attenuated in Chang liver cells. This observation may be due to its low transcriptional activity. We thus replaced the TATA box with the CMV IE1 core promoter to enhance its transcriptional activity, due to the TFIIB recognition element (RBE) residing in the CMV IE1 core promoter, in addition its TATA box sequence.[22] Indeed, the improvement successfully increased the chemiluminescence intensity 4-fold in the Chang liver cell line.

Differences in the chemiluminescence intensity between STS-treated and untreated cells were oxygen concentration dependent in a range of 0.1 to 1.0%; the lower the concentration, the stronger the intensity. There was no significant difference in the intensity at oxygen concentrations over 1.0%. In general, the median value of the oxygen partial pressure in tumor tissue is approximately 10 mmHg (1.3%), though the value would be affected by cancer cells constituting the tumor or the size of the tumor. By contrast, the median value of hypodermal tissue oxygen concentration is approximately 40–60 mmHg (5.2–7.9%).[6] It has been reported that a hypoxia-imaging agent for positron emission

tomography,[18]F-fluoromisonidazole ([18]F-FMISO), enables imaging of hypoxic regions at approximately 0.8% oxygen tension; HIF-1α proteins within tumors of the living body accumulate in areas of at least 1–3% oxygen.[23,24] Thus, with our constructed system regulated by HIF-1, we could visualize apoptosis in approximately half of the hypoxic regions in tumor tissue unaffected by normal tissue conditions. In addition, the regions visualized with[18]F-FMISO and hypoxic apoptosis regions visualized with the constructed system were predicted not to completely overlap. As we observed lower chemiluminescence intensity in Chang liver cells than in COS-7 cells, different cells could respond differently to hypoxia. Thus, even under identical conditions, hypoxic cell apoptosis might not be visualized, depending on the cell type. As we improved the transcriptional activity in this study by changing the TATA box with the CMV IE1 core promoter, we also may have to establish a simple method for fine tuning the transcriptional activity of the HRE-based promoter by changing the bases of the elements and adjusting the distances between elements.

We then employed the spheroid and successfully observed apoptosis in its hypoxic regions with our system. The spheroid is a good simulation for tumors *in vivo* since its microenvironment, including oxygen concentration, nutrition distribution, glycometabolism, and the receptor expression on the cell membrane, is similar to that of tumors.[18] It is known that hypoxic regions in tumor tissue are resistant to cancer therapies. Thus, our constructed system to visualize apoptosis, a rough therapeutic indicator, under hypoxic conditions could be a useful tool for screening anticancer agents effective in hypoxia, such as TPZ, and planning strategies for radiation therapies by determining the conditions of radiation exposure (*e.g.*, doses, timings, durations, and fractions) in a mouse tumor xenograft model implanted with 6HRE-/CMV-cLuc stable cells. Moreover, the cyclic luc system developed by Ozawa and colleagues could be a useful tool to detect apoptosis under a specific condition when applied with a specific promoter, presumably leading to the development of novel anticancer therapies. Furthermore, it is possible to image hypoxic cell apoptosis noninvasively and in real-time induced within tumors originating from living organisms, which differs from the murine tumor xenograft model implanted with 6HRE-/CMV-cLuc stable cells, by transfecting the vector which expresses the constructed hypoxic cell apoptosis imaging system to living tumor tissues. However, the *in vivo* transfection efficiency to tumors is usually quite low compared with *in vitro*. Moreover, the number of vectors delivered into hypoxic regions is predicted to be much lower due to the great distance from the blood vessel to hypoxic regions and reduced flow due to abnormal vasculature. Thus, it might be difficult to detect apoptosis within hypoxic regions due to a weak chemiluminescent signal. The development of a high-efficiency drug delivery system to hypoxic regions in tumor tissues is warranted.

Cancer stem cells (CSCs) are cancer cells that may generate tumors through the stem cell processes of self-renewal and differentiation into multiple cell types and are also considered to be the top of the hierarchy of tumor cells, similar to normal tissue stem cells. Recently, it has been realized that the hypoxic microenvironment is a key factor for stem cell phenotypes as a stem cell niche.[25] Takubo *et al.*[26] reported that hematopoietic stem cells in the bone marrow are present in the stem cell niche under the hypoxic microenvironment, suggesting that HIF-1 function is necessary to maintain the stemness of stem cells. Moreover, stem cell marker functions, such as Oct4, Nanog, Sox2, and Notch signal pathway activation by HIF, play a critical role in the mechanism for the stemness of CSCs.[27] The mechanism of stemness regulation by HIF-1 is considered to be universal in all aspects of CSCs as well as normal tissue stem cells. In the imaging system for hypoxic cell apoptosis constructed in this study, the expression of cyclic luc is regulated by HIF-1. Thus, the constructed system is anticipated to work in CSCs and considered to be available for screening of medical agents to eradicate CSCs responsible for cancer recurrence and metastasis. However, it is also known that CSCs are present in other areas than hypoxic areas.[28] Therefore, to image CSC apoptosis via mechanisms other than HIF-1, the development of another system applying the factors highly induced in CSCs is necessary.

MATERIALS AND METHODS

Reagents

All anticancer agents used in this study, such as STS, TPZ, mitomycin C, actinomycin D and doxorubicin, were purchased from Sigma-Aldrich (St. Louis, MO). These reagents were dissolved in dimethyl sulfoxide or phosphate-buffered saline (PBS) and diluted to a final concentration in culture medium. The cas-3 inhibitor Ac-DEVD-CHO was purchased from Promega (Madison, WI).

Cell culture and bacteria

COS-7 (simian cells transformed with an origin-defective mutant of simian virus 40, purchased from ATCC, Rockville, TX) and Chang liver cells (HeLa contaminant, purchased from ATCC, Rockville, TX) were grown in RPMI 1640 medium supplemented with 10%(v/v) heat-inactivated fetal calf serum, 100 U/ml penicillin and 100 µg/ml streptomycin. The cells were incubated in a 5% CO_2 incubator at 37 °C. For hypoxia treatment, the cells were incubated in a hypoxic incubator with a range from 0.1–5% O_2 balanced with N_2. The DH5 α strain of *Escherichia coli* (Takara Bio, Ohtsu, Japan) was used for the DNA manipulation experiments. The *E. coli* cells were grown in LB medium at 37 °C. All medium compositions were purchased from BD Diagnostics (Sparks, MD). All experiments with *E. coli* were performed according to the methods described by Sambrook and Russell.[29]

Plasmid constructions

To construct plasmids designated pCMV to express the cyclic luc gene from the CMV promoter, the cyclic luc gene was PCR amplified using pcFLuc-DEVD, real-time sensing plasmids for cas-3 activities constructed by Ozawa and colleagues, as the template with a combination of the following primers: a forward primer with the *Eco*RI restriction site, 5′-ATAGAATTCGCCACCATGGTTAAAG-3′ and reverse primer with the *Bam*HI restriction site, 5′-ATAGGATCCCTACACATTGATCCTAG-3′ and then inserted into the *Eco*RI–*Bam*HI site downstream of the CMV promoter in prHom-1 (Takara Bio). To explore the hypoxic-responsive promoter sequences for the expression of the cyclic luc gene under hypoxic conditions, plasmids designated p4HREs, p6HREs or p12HREs containing 4, 6 or 12 HREs upstream of the TATA box, respectively, were constructed. For the construction of plasmids p4HREs, DNA fragments containing four HREs upstream of the TATA box were PCR amplified using the plasmid p4xoptHBS as the template with a combination of the following primers: a forward primer with four copies of HRE consensus sequences, 5′-ATAACGCGTCTGCACGTACTGCACGTACTGCACGTACTGCACGTA-3′ and reverse primer, 5′-ATAACTAGTCCATTATATACCCAGATCTCGAGCCCGG-3′ and then digested with *Spe*I and *Mul*I. Underlining indicates the HRE consensus sequences. The amplified DNA fragment was ligated with a DNA fragment and PCR amplified using the pCMV as the template with a combination of the following primers to construct p4HREs: a forward primer 5′-ATAACTAGTGGATCTTGGTGGCGTGAAACT-3′ and reverse primer, 5′-GGCCATTTACCGTAAGTTATGTAAC-3′. To construct p6HREs and p12HREs, DNA fragments were PCR amplified using plasmids p4HREs as the template with the following combination of primers: a forward primer, 5′-ATAACTAGTCTGCACGTACTGCACGTACTGCACGTACTGCACGTACTGCACGTACTGCACGTAGCGGCG-3′ and reverse primer, 5′-ATAACTAGTCCTATAGTGAGTCGTATTACAATTCACTGG-3′ were self-ligated with the *Spe*I site. To construct plasmids designated p6HREs/CMV, which encodes the human CMV IE1 core promoter sequence in place of the TATA box upstream of the cyclic luc gene, DNA fragments were PCR amplified using plasmids p6HREs as the template with the following combination of primers: a forward primer with CMV IE1 core promoter sequence, 5′-ATACCTGCAGGACGTATGTCGAGGTAGGCGTGTACGGTGGGAGGCCTATATAAGCAGAGCTCGTTTAGTGAACCGTCAGATCGCGAGCTCGCCACCATGG

TTAAAGTTATCG-3′ and reverse primer, 5′-ATACCTGCAGGCAGATCTCGAG CCCGGGCTAGC-3′ were self-ligated with the *Sse*8387I site. To construct the plasmids designated pCMV/Neo and p6HREs/CMV/Neo, which encode neomycin for the selection of stable transfectants, the ampicillin resistance gene within plasmids pCMV and p6HREs/CMV was replaced with the neomycin/kanamycin resistance gene. Prior to use, the orientations, integrity, and sequences of these constructed plasmids were confirmed by nucleotide sequencing analyses.

Transfection and establishment of stable cell lines

For transient transfection experiments, 3.0×10^5 cells were seeded prior to transfection into a 60-mm glass petri dish and maintained for 12 hours at an atmosphere of 5% CO_2 at 37 °C. To evaluate the enhancement ratio of chemiluminescence by luc activity restored through cas-3 activation, the cells were transfected with plasmids pCMV, p4HREs, p6HREs, p12HREs or p6HREs/CMV using the Effectene transfection reagent (Qiagen, Valencia, CA) followed by incubation for 12 hours. For the establishment of two stably transfected cell lines, CMV-cLuc and 6HREs/CMV-cLuc, 1.0×10^6 Chang liver cells were seeded into a 100-mm culture dish and then the cells were transfected with a plasmid pCMV or p6HREs/CMV containing the neomycin/kanamycin resistance gene. Transfected cells were cultured for 14 days in culture medium containing 1 mg/ml of G418 (Nacalai Tesque, Kyoto, Japan). Antibiotic-resistant colonies were confirmed for the expression of a cyclic luc gene under normoxic and hypoxic conditions (0.1% O_2).

Spheroid culture

Stable CMV-cLuc and 6HREs/CMV-cLuc cells (2×10^5 cells per well in a 24-well plate) were seeded onto a NanoCulture Plate (Scivax, Boston, MA) for 3D cell culture. Spheroids formed after 20 days cultivation were used in this study. After adding the hypoxia probe LOX-1 (Scivax) at 4 μmol/l into the culture medium for 12 hours, hypoxic regions inside the spheroids emitting red phosphorescence were detected by observation with conventional fluorescence microscopes.

Luciferase reporter assay and *in vitro* chemiluminescent imaging of apoptotic cells

After transfection, cells were incubated in fresh medium under normoxic (20% O_2) or hypoxic (0.1% O_2) conditions for 12 hours and then treated with each anticancer agent at the indicated concentration for the indicated period. During cas-3 inhibition with Ac-DEVD-CHO, transfected cells were treated with 100 μmol/l Ac-DEVD-CHO dissolved in 0.1% dimethyl sulfoxide or vehicle (0.1% dimethyl sulfoxide only) for 1 hour prior to exposure to 1 μmol/l STS. The treated cells were washed in PBS and lysed with 100 μl of passive lysis buffer (Promega, Madison, WI) for 15 minutes at ambient temperature. The luc assay was performed using the Luciferase Assay System (Promega), following the manufacturer's instruction. Enhancement of the luc activity of each plasmid by a treatment was expressed as a fold induction where the value of luminescence by the firefly luc of a sample with the treatment was divided by that of an identically prepared sample without the treatment. Chemiluminescent dot images of a cell extract from each sample with and without treatment were acquired with a lumino image analyzer after mixing the cell extract with a luc substrate (Promega). Chemiluminescent images of apoptotic cells were acquired with a lumino image analyzer after replacing the medium containing each anticancer agent with 500 μmol/l D-luciferin (Wako, Osaka, Japan).

Western blot analysis

After treatment with 1 μmol/l STS for 2 hours, spheroids or monolayer cell cultures of stable CMV-cLuc and 6HRE-/CMV-cLuc cells were washed in PBS twice and harvested by centrifugation. The cells were lysed in 150 μl of RIPA buffer (50 mmol/l Tris-HCl pH 7.4, 400 mmol/l NaCl, 1%(v/v) Nonidet P-40, 0.25%(w/v)Na-deoxycholate) with a protease inhibitor (Sigma-Aldrich) and stored at −20 °C until use. Cell lysates (80 μg/lane) were separated through a 4–20% gradient polyacrylamide gel by sodium dodecyl sulfate-polyacrylamide gel electrophoresis and transferred onto nitrocellulose membranes (Schleicher & Schuell, Keene, NH). After blocking of the membrane with 3% skim milk in PBS for 1 hour, the membranes were incubated with anti-HIF-1α antibody (1:500, Cat#3716S, Cell Signaling Technology Japan, K. K., Tokyo, Japan) or β-actin antibody (1:1000, Cat#4970S, Cell Signaling Technology Japan, K. K) overnight at 4 °C. After washing of the membrane three times with 0.1% Triton X-100 in PBS, the membranes were incubated with horseradish peroxidase-conjugated secondary antibody for 60 minutes. The protein expression was visualized with enhanced chemiluminescence and blotting detection reagents (GE Healthcare UK, Buckinghamshire, England) using a LAS-500 luminescence imaging analyzer (GE Healthcare Japan corporation, Tokyo, Japan).

Statistical analysis

All values are expressed as the mean values ± SDs. Significant differences between groups were determined by the paired Student's *t*-test or by the unpaired Student's *t*-test. A P value < 0.05 was considered to be significant.

CONFLICT OF INTEREST

The authors declare no conflict of interest.

ACKNOWLEDGEMENTS

We thank Takeaki Ozawa (The University of Tokyo) for sharing the DNA sequence information of real-time sensing plasmids for cas-3 activities, pcFLuc-DEVD. This research was supported in part by Grants-in-Aid for Scientific Research (C) (24591849 and 26461882) from Japan Society for the Promotion of Science and by grant from Kitasato University School of Allied Health Sciences (Grants-in-Aid for Research Project, No. 2015-1031, No. 2014-1016, No. 2013-1026).

REFERENCES

1. Horvitz, HR (2003). Worms, life, and death (Nobel lecture). *Chembiochem* **4**: 697–711.
2. Guillermo, M, Mereia, N, Eric, HB and Guido, K (2014). Self-consumption: the interplay of autophagy and apoptosis. *Nat Rev Mol Cell Biol* **15**: 81–94.
3. Alenzi, FQ, Lofty, M and Wyse, RKH (2010). Swords of cell death: caspase activation and regulation. *Asian Pac J Cancer Prev* **11**: 271–280.
4. Kanno, A, Yamanaka, Y, Hirano, H, Umezawa, Y and Ozawa, T (2007). Cyclic luciferase for real-time sensing of caspase-3 activities in living mammals. *Angew Chem Int Ed Engl* **46**: 7595–7599.
5. Randy, LJ (2009). Brain tumor hypoxia: tumorigenesis, angiogenesis, imaging, psuudoprogression, and as a therapeutic target. *J Neurooncol* **92**: 317–335.
6. Brown, JM and Wilson, WR (2004). Exploiting tumour hypoxia in cancer treatment. *Nat Rev Cancer* **4**: 437–447.
7. Semenza, GL (2003). Targeting HIF-1 for cancer therapy. *Nat Rev Cancer* **3**: 721–732.
8. Lee, JW, Bae, SH, Jeong, JW, Kim, SH and Kim, KW (2004). Hypoxia-inducible factor (HIF-1) alpha: its protein stability and biological functions. *Exp Mol Med* **36**: 1–12.
9. Jiang, BH, Semenza, GL, Bauer, C and Marti, HH (1996). Hypoxia-inducible factor 1 levels vary exponentially over a physiologically relevant range of O_2 tension. *Am J Physiol* **271**: C1172–C1180.
10. Sabharwal, SS and Schumacker, PT (2014). Mitochondrial ROS in cancer: initiators, amplifiers or an Achilles' heel? *Nat Rev Cancer* **14**: 709–721.
11. Semenza, GL (2010). HIF-1: upstream and downstream of cancer metabolism. *Curr Opin Genet Dev* **20**: 51–56.
12. Wykoff, CC, Beasley, NJ, Watson, PH, Turner, KJ, Pastorek, J, Sibtain, A *et al*. (2000). Hypoxia-inducible expression of tumor-associated carbonic anhydrases. *Cancer Res* **60**: 7075–7083.
13. Feldser, D, Agani, F, Iyer, NV, Pak, B, Ferreira, G and Semenza, GL (1999). Reciprocal positive regulation of hypoxia-inducible factor 1alpha and insulin-like growth factor 2. *Cancer Res* **59**: 3915–3918.
14. Krishnamachary, B, Berg-Dixon, S, Kelly, B, Agani, F, Feldser, D, Ferreira, G *et al*. (2003). Regulation of colon carcinoma cell invasion by hypoxia-inducible factor 1. *Cancer Res* **63**: 1138–1143.
15. Dean, M, Fojo, T and Bates, S (2005). Tumour stem cells and drug resistance. *Nat Rev Cancer* **5**: 275–284.
16. Rich, JN (2007). Cancer stem cells in radiation resistance. *Cancer Res* **67**: 8980–8984.
17. Prasad, KN (1995). *Handbook of Radiobiology, 2nd edn*. CRC press, Boca Ranton, FL.
18. Robert, MS (1988). Cell and environment interactions in tumor microregions: the multicell spheroid model. *Science* **240**: 177–184.
19. Zhang, S, Hosaka, M, Yoshihara, T, Negishi, K, Iida, Y, Tobita, S *et al*. (2010). Phosphorescent light-emitting iridium complexes serve as a hypoxia-sensing probe for tumor imaging in living animals. *Cancer Res* **70**: 4490–4498.
20. Stefan, K, Milota, K and Eric, JS (2008). Rational design of minimal hypoxia-inducible enhancers. *Biochem Biophys Res Commun* **12**: 613–618.
21. Lando, D, Peet, DJ, Whelan, DA, Gorman, JJ and Whitelaw, ML (2002). Asparagine hydroxylation of the HIF transactivation domain a hypoxic switch. *Science* **295**: 858–861.

22. Butler, JEF and James TK (2002). The RNA polymerase II core promoter: a key component in the regulation of gene expression. *Gene Dev* **16**: 2583–2592.
23. Chang, J, Wen, B, Kazanzides, P, Zanzonico, P, Finn, RD, Fichtinger, G *et al*. (2009). A robotic system for 18F-FMISO PET-guided intratumoral pO2 measurements. *Med Phys* **36**: 5301–5309.
24. Harada, H, Inoue, M, Itasaka, S, Hirota, K, Morinibu, A, Shinomiya, K *et al*. (2012). Cancer cells that survive radiation therapy acquire HIF-1 activity and translocate towards tumour blood vessels. *Nat Commun* **3**: 783.
25. John, MH, Zhizhong, L, Roger, EM, Anita, BH and Jeremy NR (2009). The hypoxic microenvironment maintains glioblastoma stem cells and promotes reprograming towards a cancer stem cell phenotype. *Cell cycle* **8**: 3274–3284.
26. Takubo, K, Nagamatsu, G, Kobayashi, CI, Nakamura-Ishizu, A, Kobayashi, H, Ikeda, E *et al*. (2013). Regulation of glycolysis by Pdk functions as a metabolic checkpoint for cell cycle quiescence in hematopoietic stem cells. *Cell Stem Cell* **12**: 49–61.
27. Anfei, L, Xiya, Y and Shanrong, L (2013). Pluripotency transcription factors and cancer stem cells: small genes make a big difference. *Chin J Cancer* **32**: 483–487.
28. Christopher, C, Helen, P, Mehmet, K, Twala, LH, Christine, F, Blair, H *et al*. (2007). A perivascular niche for brain tumor stem cells. *Cancer cell* **11**: 69–82.
29. Sambrook, J, Russell, DW (2001). *Molecular Cloning: A Laboratory Manual, 3rd edn*. Cold Spring Harbor Laboratory Press, New York, NY.